On-line quality assurance of rotational radiotherapy treatment delivery by means of a 2D ion chamber array and the Octavius phantom

Ann Van Esch[a)]
Clinique Ste Elisabeth, Place L. Godin 15, 5000 Namur, Belgium
and 7Sigma, Kasteeldreef 2, 3150 Tildonk, Belgium

Christian Clermont and Magali Devillers
Clinique Ste Elisabeth, Place L. Godin 15, 5000 Namur, Belgium

Mauro Iori
Santa Maria Nuova Hospital, Viale Risorgimento 80, 42100 Reggio Emilia, Italy

Dominique P. Huyskens
Clinique Ste Elisabeth, Place L. Godin 15, 5000 Namur, Belgium
and 7Sigma, Kasteeldreef 2, 3150 Tildonk, Belgium

(Received 25 February 2007; revised 3 June 2007; accepted for publication 7 August 2007; published 17 September 2007)

For routine pretreatment verification of innovative treatment techniques such as (intensity modulated) dynamic arc therapy and helical TomoTherapy, an on-line and reliable method would be highly desirable. The present solution proposed by TomoTherapy, Inc. (Madison, WI) relies on film dosimetry in combination with up to two simultaneous ion chamber point dose measurements. A new method is proposed using a 2D ion chamber array (Seven29, PTW, Freiburg, Germany) inserted in a dedicated octagonal phantom, called Octavius. The octagonal shape allows easy positioning for measurements in multiple planes. The directional dependence of the response of the detector was primarily investigated on a dual energy (6 and 18 MV) Clinac 21EX (Varian Medical Systems, Palo Alto, CA) as no fixed angle incidences can be calculated in the Hi-Art TPS of TomoTherapy. The array was irradiated from different gantry angles and with different arc deliveries, and the dose distributions at the level of the detector were calculated with the AAA (Analytical Anisotropic Algorithm) photon dose calculation algorithm implemented in Eclipse (Varian). For validation on the 6 MV TomoTherapy unit, rotational treatments were generated, and dose distributions were calculated with the Hi-Art TPS. Multiple cylindrical ion chamber measurements were used to cross-check the dose calculation and dose delivery in Octavius in the absence of the 2D array. To compensate for the directional dependence of the 2D array, additional prototypes of Octavius were manufactured with built-in cylindrically symmetric compensation cavities. When using the Octavius phantom with a 2 cm compensation cavity, measurements with an accuracy comparable to that of single ion chambers can be achieved. The complete Octavius solution for quality assurance of rotational treatments consists of: The 2D array, two octagonal phantoms (with and without compensation layer), an insert for nine cylindrical ion chambers, and a set of inserts of various tissue equivalent materials of different densities. The combination of the 2D array with the Octavius phantom proved to be a fast and reliable method for pretreatment verification of rotational treatments. Quality control of TomoTherapy patients was reduced to a total of ~25 min per patient. [DOI: 10.1118/1.2777006]

Key words: dynamic arc, tomotherapy, quality assurance

I. INTRODUCTION

Along with the rising interest in rotational radiotherapy treatments comes the need for appropriate and efficient quality assurance (QA) solutions. Although intensity modulated arc therapy (IMAT) using all-round linear accelerators has been applied for many years now,[1–8] its use has mostly been restricted to academic centers having developed their in-house solution for the planning as well as for the QA. In general, a phantom approach is used for the treatment verification: The treatment plan is transferred onto a phantom, and the dose is recalculated for this phantom setup. Measurements are performed mostly with film (radiographic or radiochromic)[9–12] and ion chamber point dose measurements.[13] Gel dosimetry was also shown to be of interest.[14,15] With the commercial availability of the helical TomoTherapy solution,[16–20] the rotational IMRT treatments are becoming available to a wider range of radiotherapy centers. Many of these, however, lack the time and personnel for time consuming patient specific QA. As the rotational treatments are still innovative and suffering from growing pains, patient specific QA remains advisory and the need for fast and reliable QA tools is therefore imminent. TomoTherapy includes a QA package within their treatment solution,[21–23] relying on film dosimetry in combination with up to two simultaneous ion chamber point dose

measurements. Although film dosimetry is a valuable, well established QA method when performed correctly, its reliability heavily depends on the constancy of external parameters such as the quality of the dark room and the stability of the film developer and on the possibility to correct for artifacts related to the scanner. Because of the increased use of digital imaging in radiology and radiotherapy, well monitored, stable film developers are becoming more and more difficult to find in the average hospital environment. The circular phantom—referred to as the Cheese phantom—designed for TomoTherapy QA purposes has a length of 18 cm, which is not sufficient to cover most head and neck treatment plans within one verification setup. For machine QA, the TomoDOSE diode array (Sun Nuclear, Melbourne, FL) can be purchased to provide on-line data on the reproducibility of the beam profiles in static gantry mode,[24] but it cannot be used for TPS validation or patient pretreatment verification.

Portal dosimetry remains by far the most time efficient pretreatment verification method for fixed gantry IMRT treatments, provided it is fully integrated in the used IMRT solution.[25–27] Although it is not yet commercially available for (intensity modulated) dynamic arc treatments, in theory, both the image acquisition and prediction should be very similar to the fixed gantry portal dosimetry solution. No portal imager is available on the TomoTherapy treatment unit, but the linear detector array used for the acquisition of the MV-CT could potentially be used for measuring the dose delivery during irradiation. However, both image acquisition modalities show the considerable disadvantage that they rotate along with the treatment beam and will therefore not include any angular information in their data acquisition. In extremis, should the treatment beam not rotate at all during delivery, this will go undetected in the portal image acquisition. Although portal dosimetry may eventually be part of a QA solution including additional monitoring of the gantry angle, pretreatment verification in a phantom remains the most complete verification method for now.

In order to replace the film measurement with a less troublesome, absolute and preferably on-line 2D dose measurement method, the applicability of the Seven29 (PTW, Freiburg, Germany) 2D ion chamber array[28,29] was investigated. In addition, a multipurpose phantom was developed to overcome some of the disadvantages of the Cheese phantom while accommodating for the use of the ion chamber array in multiple measurement planes. The Seven29/Octavius combination was validated for use on a Clinac as well as on a helical TomoTherapy treatment unit.

II. MATERIAL AND METHODS

Although the goal of the study is to use the detector during any kind of dynamic rotational treatment to investigate its directional dependence, most of the initial tests were performed by means of static fields and simple arc treatments on a dual energy (6 and 18 MV) linear accelerator Clinac 21EX (Varian Medical Systems, Palo Alto, CA). It was then verified if the data obtained on the TomoTherapy 6 MV treatment unit were consistent with that obtained on the Clinac.

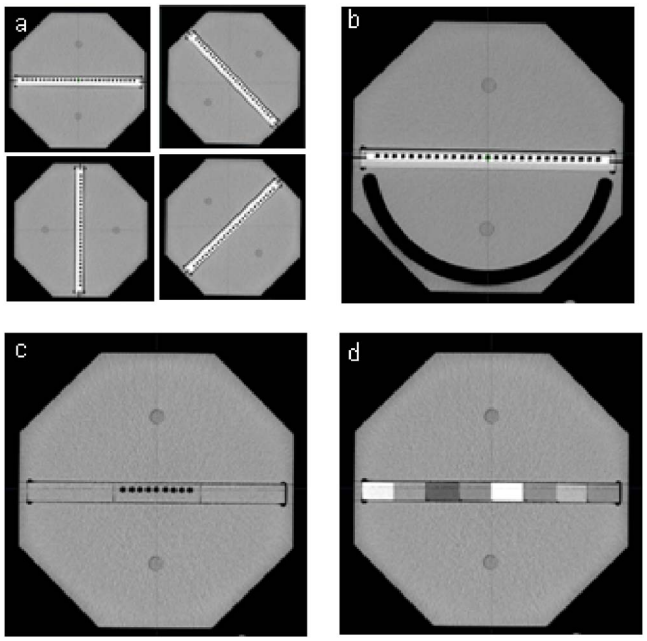

FIG. 1. Different configurations of the Octavius phantom: (a) Octavius$^{CT\text{-}IC}$ with 2D array for dose calculation in different planes of measurement, (b) Octavius^{729}/2D array tandem for measurements, (c) Octavius$^{CT\text{-}IC}$ with multiple ion chamber insert, and (d) Octavius$^{CT\text{-}IC}$ with heterogeneous inserts.

Following its validation, the newly developed QA procedure was tested on a number of dynamic arc and TomoTherapy patients.

II.A. The Octavius phantom

A dedicated phantom was constructed for the QA of rotational treatments focusing primarily on the use of the Seven29 (PTW, Freiburg, Germany) 2D ion chamber array, but also allowing individual ion chamber measurements. An octagonal shape was chosen to allow data acquisition in multiple planes with an easy phantom setup. The phantom is called Octavius and is made of polystyrene (physical density 1.04 g/cm^3, relative electron density 1.00). It is 32 cm wide and has a length of 32 cm. A $30\times30\times2.2$ cm^3 central cavity allows the user to insert the 2D ion chamber array into the phantom [Fig. 1(a)]. The position of the cavity is such that when the 2D array is inserted, the plane through the middle of the ion chambers goes through the center of the phantom. For the single ion chamber measurements, three separate slabs of $10\times31\times2.2$ cm^3 were constructed [Fig. 1(c)], two of which are entirely solid whereas the third slab contains nine ion chamber inserts with a center to center spacing of 1.05 cm and a diameter of 0.69 cm to accommodate for 0.125 cc thimble chambers (T31010 Semiflex, PTW, Freiburg, Germany). The nine thimble chambers can be read out simultaneously by means of the Multidose electrometer (PTW, Freiburg, Germany) equipped with a connector box.

In addition, inserts of different tissue equivalent materials (Barts and The London NHS Trust, London) [Fig. 1(d)] al-

low point dose verification of the calculated dose in and near heterogeneities. They can also be used for the Houndsfield unit calibration of the CT and MV-CT.

II.B. The 2D ion chamber array

The detector used for this study is the Seven29 2D ion chamber array (PTW, Freiburg, Germany), consisting of 27 $\times$ 27 vented cubic ion chambers of $0.5 \times 0.5 \times 0.5$ cm^3 each, with a center to center spacing of 1 cm. The upper electrode layer is positioned below a 0.5 cm PMMA build-up layer; the lower electrode layer lies on top of a 2 mm thick electrode plate, which is again mounted on a 10 mm PMMA base plate. The 5 and 10 mm PMMA layers have a water equivalent thickness of 0.59 and 1.18 cm, respectively. The original electrometer, which was potentially subject to signal saturation during the high dose rate delivery that is typical for TomoTherapy, was replaced by the more recent array interface that can handle up to 16 Gy/min. The 2D array is calibrated for absolute dosimetry in a ^{60}Co photon beam at the PTW secondary standard dosimetry laboratory. This dosimetric calibration is a fully automated procedure during which the array is mounted in front of the ^{60}Co source and mechanically moved in small steps in the $x-y$ direction. Every chamber is moved into the central calibration position and irradiated during a fixed time interval. As such, a matrix of calibration factors relative to the central chamber is made. Finally, an absolute calibration is performed for the central chamber assuming the effective point of measurement to be at 5 mm below the array surface. The manufacturer recommends a recalibration every two years. The use of the array for rotational treatment delivery was validated by means of comparison to dose calculations and single ion chamber measurements of different vendors.

II.B.1. The effective point of measurement

In order to investigate the position of the effective plane of measurement in the 2D array as a function of gantry angle, the effective plane of measurement was first determined for gantry angles 0° and 180°, i.e., for normal beam incidences from the front and from the rear. For this, we used a similar method as proposed by Poppe *et al.*:[29] By placing increasing amounts of solid water (Gammex RMI, Cablon Medical, The Netherlands) on top of the array, depth dose curves were measured for a 10×10 cm^2 field for SPD=100 cm, for 6 and 18 MV. Each data point was acquired with 100 MU. The effective measurement depth was derived from comparison with depth dose curves obtained with an ion chamber (RK 0.12 cm^3, Wellhofer Sanditronix, Germany) in water.

II.B.2. Directional dependence

CLINAC

To be able to evaluate the accuracy of the absolute dose measurement as a function of beam angle, as a first step, the overall dose absorption of the 2D array as an entity was characterized. The array was placed 5 cm below and on top of 10 cm of solid water material. A large diameter ion chamber (NACP, Wellhofer Scanditronix, Germany) was inserted in the solid water at 5 cm below the 2D array. The ion chamber readout was measured for field sizes 10×10, 15×15, and 20×20 cm^2 (200 MU), for 6 and 18 MV. The measurements were repeated with the 2D array replaced by solid water of the same physical thickness.

The initial validation of the directional dependence was done mostly by means of static field deliveries. The isocenter was placed in the center of Octavius; this also being the middle of the central ion chamber. To exclude all effects that could originate from irradiation through the treatment couch, instead of rotating the gantry from 0° to 180° around Octavius with a horizontally placed 2D ion chamber array, the phantom was turned such that the array was in the vertical (sagital) plane, and data were acquired for gantry angles going from 90° to 270° (CCW) in steps of 15°. Gantry 90° and 270° correspond to orthogonal beam incidence from the front and rear of the array, respectively. For clarity, however, we will refer to these as if the array were in its horizontal position and report on gantry angles going from 0° to 180°. Temperature, air pressure, and daily output fluctuations were monitored and corrected for.

Data were acquired for a square field size of 10×10 cm^2 and 15×15 cm^2 (100 MU), for 6 and 18 MV. The dose distribution for each field was also calculated on the CT scan of the phantom setup by means of the AAA (analytical anisotropic algorithm) dose calculation algorithm in Eclipse (Varian Medical Systems, Palo Alto, CA). We used the AAA dose calculation algorithm because it was reported to be more accurate than the Pencil Beam Convolution (with the Modified Batho heterogeneity correction),[30] and because it was found to yield comparable results to the superposition/convolution[31–35] dose calculation algorithm, the latter being used in the Hi-Art TPS. The dose in the plane of measurement was exported in dicom format for comparison in the VERISOFT (PTW, Freiburg, Germany) software, used for acquiring and analyzing the 2D array data.

Following the static field validation, a number of rotational test plans were performed. As the purpose of these tests was the development of a reliable measurement procedure rather than the actual validation of the dose calculation or dynamic leaf movement, treatment plans have been restricted to geometrically simple deliveries, for which a high level of confidence can be placed on the dose calculation. On the Clinac, open field dynamic arc treatments were delivered for various open field sizes (6×6, 10×10, 15×15, 20×20 cm^2), for 6 and 18 MV. Irradiation through the couch was again omitted by restricting the gantry rotation from 270° to 90° (CW) and using the vertical (sagital) setup. With this setup, all beam incidences are equally well covered. Temperature, air pressure, and daily output fluctuations were again corrected for.

TOMOTHERAPY

As a consistency check, a number of static fields of 2.5×25 cm^2 were delivered for the fixed gantry angles on the TomoTherapy 6 MV treatment unit. Static field delivery is only possible at 0°, 90°, 180°, and 270°. To avoid any influ-

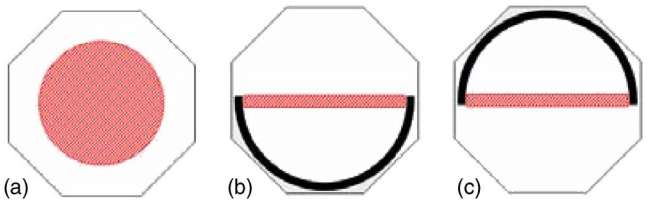

FIG. 2. Schematic of the structures used for generating the TomoTherapy test plans. The circular structure in (a) is used to generate a uniform, cylindrical dose delivery. When optimizing on the rectangular PTV (b) and (c), the half cylinders are used as directional blocks, i.e., to avoid beam delivery from (b) the rear and (c) from the front.

ence from the table, to exclude any machine output dependence as a function of gantry angle and to obtain at least two oblique incidences (45° and 135°), instead of applying a gantry rotation the phantom was turned onto its different outer surfaces [cf. Fig. 1(a)]. Although some static fields can be programmed on the TomoTherapy treatment unit, the Hi-Art treatment planning system does not support dose calculation of these beams. Hence, no comparison of dose calculation versus measurement is possible for static fields. Therefore, in addition, three TomoTherapy plans were generated with the Hi-Art TPS. As the TPS takes the presence of the treatment couch into account in the dose calculation, these tests were performed with the array in the horizontal position. The CT scans of the phantom setups were acquired such that the central axis of Octavius coincided with the central axis of the TomoTherapy treatment unit in the Hi-Art TPS. The structures used for the creation of these test plans are schematically outlined in Fig. 2. A central cylinder [Fig. 2(a)] of 20 cm diameter, 15 cm in length was contoured on the CT of the Octavius phantom (in which the array had been replaced by solid inserts of the same material as the phantom itself). A TomoTherapy treatment was optimized to yield a homogeneous dose of 1 Gy to this cylinder. Three additional structures were contoured: A rectangular target with the same size and position as the array and two artificial C-shaped structures at the outer edge of the phantom, one in the lower [Fig. 2(b)] and one in the upper [Fig. 2(c)] half. During the optimization, a homogeneous dose of 1 Gy was requested to the rectangular target, while demanding a directional block on the lower and upper C-shaped structure, respectively. All plans were transferred to the Octavius phantom with the array in its horizontal (coronal) position, and the dose plane through the center of the array was exported for comparison with measurements. In addition, the correct delivery of the plan was cross-checked with cylindrical ion chambers by means of a treatment verification plan on the Octavius phantom with the multiple ion chambers insert [Fig. 1(c)]. No line profile export or 2D/3D dicom dose export exists in the currently available clinical version of the Hi–Art TPS. By playing along with the in–built procedure for film dosimetry, however, an ascii or binary planar dose export filter can be made available. Pretreatment patient plan verification is performed on-line in the VERISOFT software. All 1D line profiles used in this article (e.g., for comparison with the multiple ion chamber measurements) were obtained by first using the 2D dose ascii export and subsequently extracting the line profile using the VERISOFT software.

II.C. The Octavius^{729}/2D array QA tandem

A modified Octavius was constructed for the actual measurement with the Seven29 ion chamber array. This phantom is an identical copy of the above described Octavius (further referred to as Octavius$^{CT\text{-}IC}$), except that it has a built-in cylindrically symmetric compensation cavity to correct for anisotropic behavior of the 2D ion chamber measurements [Fig. 1(b)]. Two prototypes with different compensation cavity thickness (1.6 and 2 cm, respectively) were constructed. These phantoms are referred to as Octavius$^{729}_{16}$ and Octavius$^{729}_{20}$, respectively. The same tests as described in Sec. II B were repeated on these phantoms.

II.D. Pretreatment QA

CLINAC

Daily machine output verification

At the beginning of every pretreatment QA session, the Octavius^{729}/2D array tandem is irradiated with a 10 $\times$ 10 cm^2 open field with 156 MU for 6 MV and 120 MU for 18 MV (Gantry=0°, source phantom distance SPD =84 cm). For our specific Clinac calibration, this should correspond to a dose of 1 Gy in the isocenter, i.e., at the effective point of measurement of the array. Three successive measurements are performed per energy. After having been corrected for temperature, air pressure, and energy dependence, they provide us with the daily machine output fluctuation. Provided the measurements are stable (within 0.2%) and the observed output fluctuation is within tolerance (within 2% of the nominal value), an additional correction factor is extracted to eliminate the effect of the machine output during the rest of the QA session.

Pre-treatment patient QA

To assess the use of the Octavius^{729}/2D Array tandem for the quality assurance of dynamic arc delivery, a number of arc treatments were generated by means of the "fit and shield" tool in the Eclipse TPS. For a given arc, the "fit and shield" option fits the MLC around the PTV(s) with a given margin, while shielding the selected organs at risk. Although the PTV dose coverage and organ sparing in these plans are expected to be inferior to what can be obtained by means of inverse planning IMAT, the procedure for plan verification could be identical. Dynamic arc plans were made on five prostate (18 MV), four rectum (18 MV), and three head and neck (6 MV) patients. To avoid irradiation through the treatment couch, the arc movement was restricted between 235° and 125°. All plans were verified by means of the Octavius^{729}/2D Array tandem as well as by means of multiple ion chamber measurements in the Octavius$^{CT\text{-}IC}$ phantom. Data were acquired in the horizontal as well as in the vertical plane. TPS dose calculations were performed on a CT scan of the phantom with the 2D array [Fig. 1(a)] as well as with the multiple ion chamber insert (Fig. 1(c)).

TOMOTHERAPY

Daily machine QA

As the technology of the TomoTherapy unit is still very new, every patient QA session was preceded by a compact daily QA procedure on Octavius to monitor the most important machine characteristics and to allow distinction between general and patient specific discrepancies. This daily QA procedure focuses only on the machine characteristics that would have an immediate and potentially significant impact on the treatments. First, as phantom/patient positioning heavily relies on the accuracy of the moveable lasers as well as on the MV-CT acquisition and registration procedure, these are the first items to be checked. For this, an MV-CT is acquired of the Octavius phantom containing a number of heterogeneous inserts. This image set is used to check the position of the moveable and fixed lasers, to verify the registration procedure, and to simultaneously monitor the stability of the HU calibration curve for the MV-CT. Second, the cylindrical target delivery on the Octavius^{729}/2D Array tandem as described in Sec. II B 2 is used as a surrogate for daily dosimetry (i.e., machine output), but inherently verifies the correct couch movement as well. At least two successive measurements (of 326 s beam-on time each) are taken to monitor the output stability of the treatment unit.

Pretreatment patient QA

The developed procedure for pretreatment QA in routine was tested on a cohort of 20 patients (15 head and neck, 4 prostate, and 1 brain lesion) on the TomoTherapy treatment unit. For all 20 patients, QA plans were calculated on Octavius$^{\text{CT-IC}}$ (and delivered to Octavius$^{729}_{20}$) for both orthogonal array positions. For a limited number of patients, a QA plan was also generated on the phantom setup with the multiple ion chamber insert. Although the simultaneous use of nine ion chambers considerably speeds up the measurements process, each set of nine data points takes 10 to 15 min to measure (depending mostly on the beam-on time of the plan), leading to a total measurement time of 60 to 90 min per patient for two orthogonal line profiles. Therefore, this validation procedure was only performed for five patients. Temperature and air pressure were corrected for during every measurement. The 2D dose planes were exported from the TPS and imported into the VERISOFT software prior to delivery to allow on-line verification.

All 2D patient data were analyzed by means of the gamma evaluation in the VERISOFT software. The gamma index method is based on the theoretical concept of Low *et al.*,[36] using the approach of Depuydt *et al.*[37] to take into account practical considerations concerning the discrete nature of the data. The 2D array measurement data is always used as a reference matrix for the gamma calculation, and the TPS data are automatically interpolated by the software to a grid size of 0.5 mm. As acceptance criteria, we applied a fixed value of 3 mm for the distance to agreement (DTA) and dose difference tolerance levels of 1% to 5% (of the local dose value). Values below 5% of the maximum dose are ignored in the analysis.

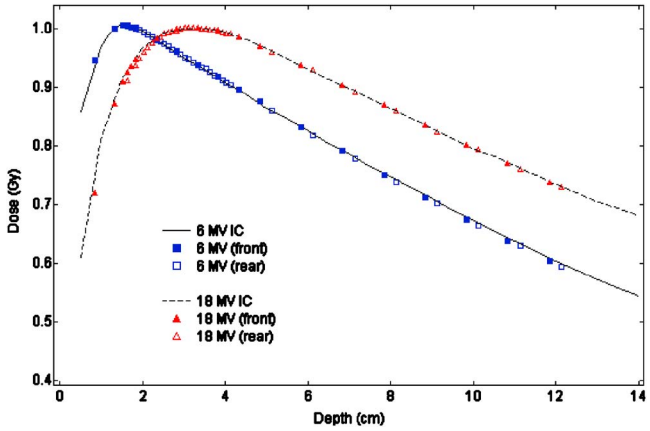

FIG. 3. Absolute depth dose measurements obtained for a 10×10 cm^2 field with a single ion chamber in water [solid (6 MV) and dashed (18 MV) line] (SPD=100 cm, 100 MU). Data measured with the central ion chamber of the 2D array in solid water were shifted and renormalized to coincide with the absolute measurements in water. Filled and open markers correspond to array irradiation from the front and from the rear, respectively.

III. RESULTS

III.A. The 2D ion chamber array

III.A.1. The effective point of measurement

A comparison between the depth dose curves obtained with an ion chamber in water and with the array by means of solid water plates is shown in Fig. 3 for 6 and 18 MV. The ion chamber measurements in water are displayed in absolute dose as they have been normalized to an absolute point dose measurement at 5 cm depth for 100 MU. For the depth dose curves measured with the central ion chamber of the 2D array, the displayed data have undergone two manipulations. First, when assuming this depth to be the sole sum of the solid water and detector material covering the ion chambers (i.e., 0.59 cm for irradiation from the front, 1.38 cm for irradiation from the rear), it was found that an additional shift of 0.25 cm needed to be applied (for both incidences and for both energies) to obtain the same depth of dose maximum as measured with the ion chamber in a water tank. Second, after having applied this shift, a small correction factor (0.981 for 6 MV, 0.985 for 18 MV) needed to be applied to obtain the same level of absolute dose when irradiating from the front. The depth dose data obtained when irradiating the array from the rear showed a considerably larger absolute difference, as will be discussed below, and have been normalized to the same absolute dose at 5 cm depth as the ion chamber measurements in water. The absolute dose correction when irradiating from the front is linked to the fact that the effective point of measurement for the 2D ion chamber array was thought to be at the level of the upper electrode during the original absolute calibration of the device. With the newly found information, energy dependent correction factors for the absolute dosimetry were again derived by means of a cross calibration with the local reference thimble ion chamber (NE 2571) in solid water at the Clinac. The thus derived correction factors were $k_{6\ \text{MV}}=0.981$ and $k_{18\ \text{MV}}=0.985$, in excellent agreement with the correction factors found from

the depth dose behavior. This calibration correction was taken into account for all further measurements.

III.A.2. Directional dependence

CLINAC

The absolute dose measured in the solid water at 5 cm below the array was within 1.5% of the absolute dose measured in the same configuration but with the array replaced by a 2.2 cm solid water slab, showing that the overall dose absorption of the array is near water equivalent.

The directional dependence of the 2D ion chamber array can be observed in Fig. 4(a), showing the measured and calculated profiles for a 10×10 cm^2 field for a number of gantry angles (gantry 0°, 30°, 60°, 90°, 120°, 150°, and 180°). Figure 4(b) shows the percentage dose difference on the beam axis as a function of gantry angle. When the array is irradiated from the front, agreement between TPS and measurement is within 1.0% on the beam axis and within 2%, 2 mm over the whole measured surface, for both energies, even for highly oblique incidences. However, when the beam incidence moves to the rear of the array, a considerable absolute deviation becomes apparent. When measured and calculated data are both normalized to their value on the beam axis, agreement is restored to within 2%, 2 mm. Apart from a narrow transition period for gantry angles between 75° and 105°, the percentage dose difference quickly saturates onto the constant value of 4% for 18 MV and 8% for 6 MV. Whereas the TPS is predicting only slight differences between the absorbed doses for mirrored beam angles (e.g., 45° and 135°), measurements for gantry angles between 90° and 180° show a considerably smaller signal. Very similar results to the ones displayed in Fig. 4 were obtained for the other field sizes: All showed a relative overall agreement of 2%, 2 mm when normalized to the beam axis and a percentage dose difference as displayed in Fig. 4(b).

For all field sizes, the correct delivery of the half-arc open field treatment was confirmed by means of the multiple ion chamber measurements (Fig. 5). There is a noticeable difference between the dose calculation on the Octavius$^{\text{CT-IC}}$ phantom with the 2D array and with the multiple ion chamber insert because of their different structure and average density. Separate dose calculations for both setups are therefore required. For the multiple ion chamber measurements, in theory, the dose should be recalculated for all three possible positions of the ion chamber insert. We have, however, performed only a single dose calculation on the phantom with the insert in its central position. From Fig. 5, it appears that this is an adequate approximation for the overall line profile calculation during arc delivery. Knowing the arc delivery to be correct, in Fig. 5 we observe that the array measurement underestimated the dose on the beam axis for the open field half-arc treatment deliveries by 4% for 6 MV and 2% for 18 MV.

TOMOTHERAPY

Similar discrepancies as the ones observed between mirrored field incidences for the 6 MV Clinac treatment beam, were observed for the static field deliveries on the TomoTherapy treatment unit (not shown). The results obtained on the Clinac were also confirmed by the three test plans generated with the TomoTherapy TPS, although the data interpretation is hampered by additional discrepancies observed. First, as will be illustrated in Sec. III C (Fig. 7 below), output fluctuations of up to 2% between successive measurements are commonly observed on our TomoTherapy treatment unit. In an effort to exclude these from the final data, all displayed data are averaged over multiple measurements. Secondly, the TPS predicts a homogeneous dose delivery over the whole cylinder whereas both the multiple ion chamber measurements and the 2D array data show a dip in the center of the profile. Between the dose calculated for the multiple ion chamber setup and the actual measurement, a ~4% underdosage is detected in the center of the TomoTherapy unit, gradually improving to ~2% at an off-center distance of 2 cm and finally converging towards the calculated data at ~7 cm off-center distance. To exclude all possible effects from the Octavius phantom construction, as a triple check, the treatment plan was transferred onto the Cheese phantom, and a horizontal line profile was measured by means of point by point ion chamber measurements with the standard ion chamber included in the TomoTherapy QA package (A1SL, Standard Imaging, Middleton, WI). The results were very similar to the results displayed in Fig. 6(a). In addition to the discrepancies in the profile shape, the 2D array measurement in Octavius$^{\text{CT-IC}}$ displays a ~4% general dose underestimate. The 2D array data from the test plan solely irradiating from the front [Fig. 6(b)] show similar overall agreement as the multiple ion chamber data, both again deviating from the calculated profiles by a dip of ~4% around the center. Ignoring the central deviation, the test plan solely allowing irradiation from the rear [Fig. 6(c)] shows an overall dose underestimate of ~7%, in agreement with the findings on the Clinac for 6 MV.

III.B. The Octavius^{729}/2D array QA tandem

Measurements obtained for the 10×10 cm^2 field irradiation of the 2D array in Octavius$^{729}_{20}$ are displayed in Fig. 4(a) for different gantry angles. As can be seen from Fig. 4(b), the 16 mm compensation cavity of Octavius$^{729}_{16}$ reduces the deviation on the beam axis for irradiation from the rear to a maximum of 3% for 6 MV and 1.7% for 18 MV for gantry angles between 105° and 180°. For these gantry angles, data obtained with Octavius$^{729}_{20}$ are within 1.5% of the calculated dose on the beam axis. Since the compensation cavity does not extend to the side of the array [cf. Fig. 1(b)], the discrepancy between calculation and measurement remains unaltered for sidewise beam incidence. As the 20 mm cavity offers the better compensation for the directional dependence of the array for both energies, only results on Octavius$^{729}_{20}$ will be shown in the rest of this work.

Figure 5 illustrates the results obtained for a 10×10 cm^2 half-arc for 6 and 18 MV. On the beam axis, Octavius$^{729}_{20}$ reduced the discrepancy to ~1% for 6 MV and to less than 0.5% for 18 MV. A 2%, 2 mm overall agreement was achieved for both energies.

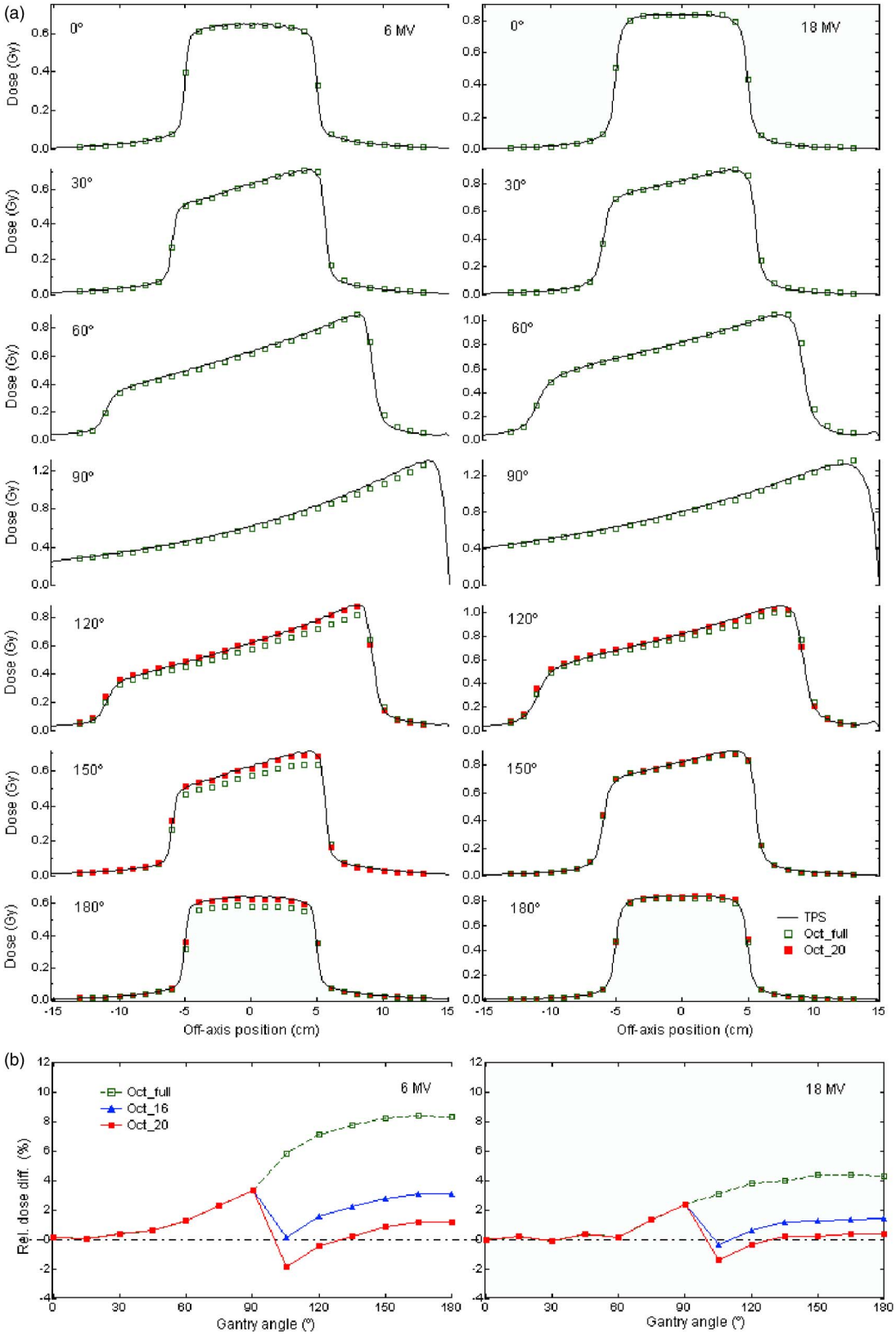

FIG. 4. (a) Absolute cross-plane dose profiles calculated (AAA) and measured (2D array) in Octavius for 6 and 18 MV. Measurements obtained in the Octavius$^{CT\text{-}IC}$ phantom are indicated as Oct_full, while Oct_16 and Oct_20 correspond to the measurements in the Octavius phantoms containing a 16 and 20 mm compensation cavity, respectively. All dose calculations (solid lines) were performed on the CT scan of the full Octavius$^{CT\text{-}IC}$ phantom. (b) Relative dose difference between calculation and measurement on the beam axis for the different measurement setups.

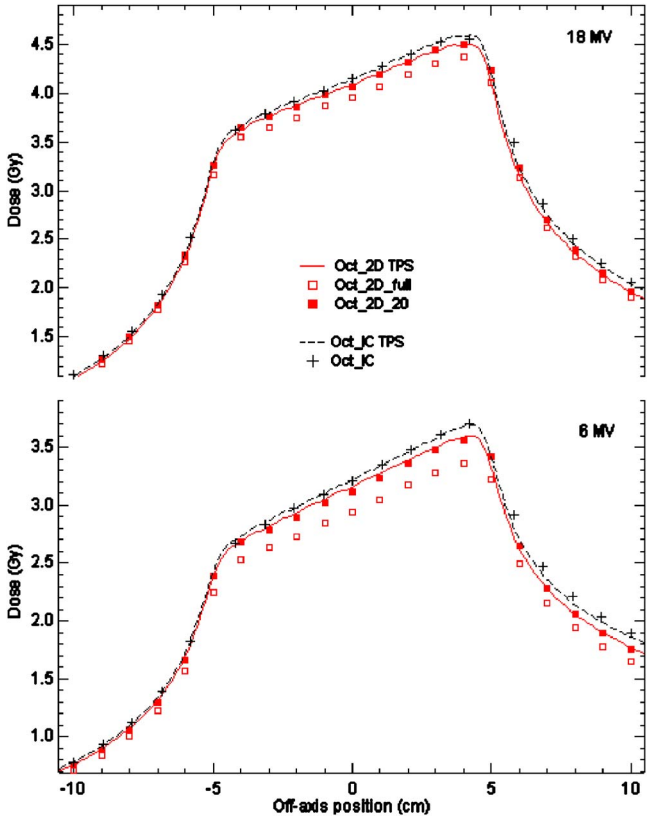

FIG. 5. Measured and calculated half-arc delivery for a 10×10 cm^2 field size for a 6 and 18 MV treatment beam (500 MU). Array measurements obtained in the full Octavius$^{CT\text{-}IC}$ phantom are indicated as Oct_2D_full. Oct_2D_20 corresponds to the measurements in the Octavius phantoms containing a 20 mm compensation cavity. Data obtained with the individual ion chambers are indicated as Oct_IC. All dose calculations (solid and dashed lines) were performed on the CT scan of the full Octavius$^{CT\text{-}IC}$ phantom, containing the 2D array (Oct_2D TPS) or multiple ion chamber insert (Oct_IC TPS).

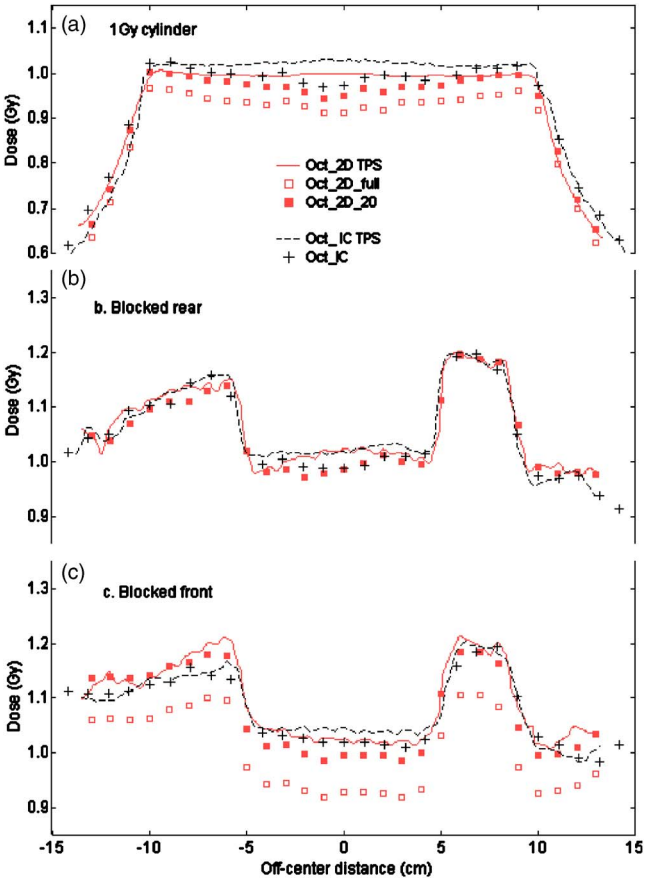

FIG. 6. Measured and calculated treatment verification plans on the TomoTherapy treatment unit. A homogeneous dose delivery of 1 Gy to a central cylinder was the planning objective in (a); (b) and (c) illustrate results obtained for a treatment plan prohibiting irradiation from the rear and front of the array structure, respectively. Measurements obtained with the 2D array in the full Octavius$^{CT\text{-}IC}$ phantom are indicated as Oct_2D_full; Oct_2D_20 corresponds to the measurements in the Octavius phantoms containing a 20 mm compensation cavity. Data obtained with the individual ion chambers are indicated as Oct_IC. All dose calculations (solid and dashed lines) were performed on the CT scan of the full Octavius$^{CT\text{-}IC}$ phantom, containing the 2D array (Oct_2D TPS) or the multiple ion chamber insert (Oct_IC TPS).

Data obtained for the validation of the Octavius^{729}/2D Array QA combination on the TomoTherapy treatment unit, are superposed on the graphs in Fig. 6. Figures 6(a) and 6(c) illustrate the considerable improvement in the measurement data with the use of Octavius$^{729}_{20}$. Octavius$^{729}_{16}$ provides similar, albeit slightly inferior results (not shown). The line profiles obtained for the cylindrical test plan shown in Fig. 6(a) now show the same discrepancies as the multiple ion chamber data when compared with the dose calculated by the TPS.

III.C. Pretreatment QA

CLINAC

First, Fig. 7 shows typical results obtained during the daily machine monitoring procedure at the start of the patient QA session. The day-to-day output variations on the Clinac are smaller than 1% and differences between consecutive measurements during the same QA session are smaller than 0.2%. The stability of the beam allows us to correct for the machine output by means of a simple cross calibration.

For the dynamic arc deliveries on the Clinac, all measurements agreed with the calculations within 3%, 3 mm for nearly all measurement points encompassed by the 50% isodose line. Figure 8 shows typical results for a rectum (18 MV) and head and neck treatment (6 MV), respectively. The squares on the isodose overlays indicate points that failed the gamma criteria. The doses measured with the multiple ion chamber inserts are generally about 2% higher than the doses measured with the array but correspond equally well to their calculated counterparts.

TOMOTHERAPY

As can be seen from Fig. 7, the output stability of the TomoTherapy was found to be of the order of 1%–2% for day-to-day as well as for intrasession consecutive measurements. Because of the latter, no correction for daily output variation can be applied to the subsequent patient QA plan delivery in clinical routine. Figure 9 shows typical results obtained with the pretreatment QA procedure in the coronal [Figs. 9(a) and 9(b)] and sagital [Fig. 9] plane on the TomoTherapy unit. For the data displayed in Fig. 9—as an alter-

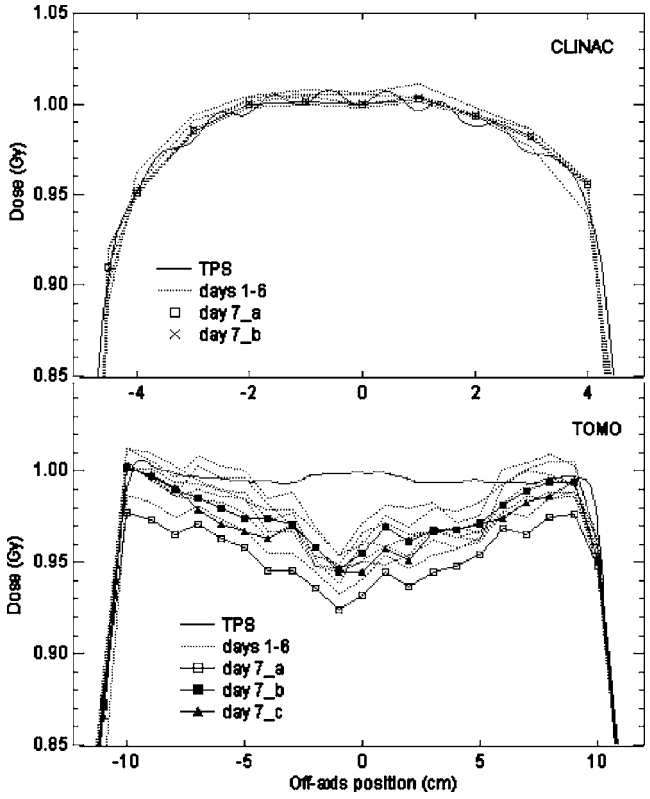

FIG. 7. Typical output variations as observed with a 10×10 cm^2 reference field on a Clinac (6 MV) and with the cylindrical dose delivery on the TomoTherapy unit. For each treatment unit, day to day (days 1–6) as well as successive measurements on the same day (day 7_a, day 7_b, …) are displayed.

native to the machine output correction on the Clinac—several consecutive measurements were done and averaged prior to analysis. In the Hi-Art software, it is not trivial to move the phantom to the exact same location for different QA setups. Small positional shifts will result in slightly different line profiles calculated for the array and the multiple ion chamber setup. This can be observed in the upper part of Fig. 9 and in the plot of the corresponding line profiles. However, both QA setups show consistent agreement between measurement and calculation. When the PTV is located near the center of the TomoTherapy unit, similar discrepancies as described for the cylindrical test plan appear. Figure 9 shows an example of such a prostate treatment plan: An underdosage of more than 3% is observed in the center of the target, and gamma evaluation tolerance levels have to be increased to 5%, 3 mm to obtain overall agreement within the 50% isodose level. This underdosage is not observed for the treatment plans for which the PTV is off-center, as is the case for most head and neck patients treated on the TomoTherapy unit in our department: 3% 3 mm acceptance criteria could be met for nearly all measurement points within the 50% isodose line. For routine patient QA, it is not feasible to average the data out over multiple acquisitions, and, although acceptance criteria of 3% 3 mm can still be met for a number of 2D data, a considerable fraction of the 2D images requires 5%, 3 mm tolerance levels. For the remaining 18 patients, a total of 36 data sets was analyzed: For 14 of those, the 3%, 3 mm criteria were met for nearly all data points within the 50% isodose, 21 data sets required tolerance levels of 5%, 3 mm, 1 data set did not meet the 5%, 3 mm criteria. The latter was found to be a prostate patient with a similar discrepancy as shown in Fig. 9(a) and a 2% too low machine output. By repeating the 2D dose acquisition, data with a higher machine output were obtained and the 5%, 3 mm criteria could be met.

IV. DISCUSSION

IV.A. The Octavius phantom

Although a Cheese phantom is available for QA measurements and the array can be sandwiched between the two halves of the Cheese phantom, the main motivations behind the construction of Octavius were the fact that the Cheese phantom is too short (18 cm) to fit in most head and neck treatment plans and the fact that nonhorizontal positions are not easy to set up and even hold a significant risk of damage for both the array and the phantom. The Octavius phantom allows the full use of the 27×27 cm^2 array surface for measurements and proved very easy to set up for multiple orientations of the measurement plane. As a disadvantage, although the width is comparable to the diameter of the cheese phantom, the additional length increases the weight of the phantom to a total of ~25 kg. The cavity foreseen for the array in Octavius is of such dimensions that a variety of inserts—such as ion chamber and heterogeneous inserts—can be manufactured, converting it into a multipurpose phantom. The Octavius phantoms were constructed in collaboration with PTW (PTW Freiburg, Germany) and will be made commercially available by the latter.

IV.B. The 2D ion chamber array

For a typical plane parallel ion chamber, the effective point of measurement is situated very near to the entrance surface of the chamber because of the large diameter of the planar electrode compared to the distance between the electrodes and because of the surrounding guard ring. Although the ion chambers in the PTW729 ion chamber array consist of two plane parallel electrodes, the distance between the electrodes is equal to their width (i.e., 0.5 cm). The grid between the ion chambers limits cross talk, but its construction is different from that of a standard guard ring. As such, the effective point of measurement for the 2D array ion chambers was found not to lie at the entrance electrode but in the middle of the chamber. When using only the 2D ion chamber array for field by field measurements with perpendicular beam incidence from the front of the array, the exact location of the effective point of measurement is less critical than in a 3D dose delivery. Assuming the effective point of measurement to lie at the level of the upper electrode has no considerable impact on the accuracy of the measurement method when the same effective point of measurement is assumed during calibration; a slight error in this location will almost

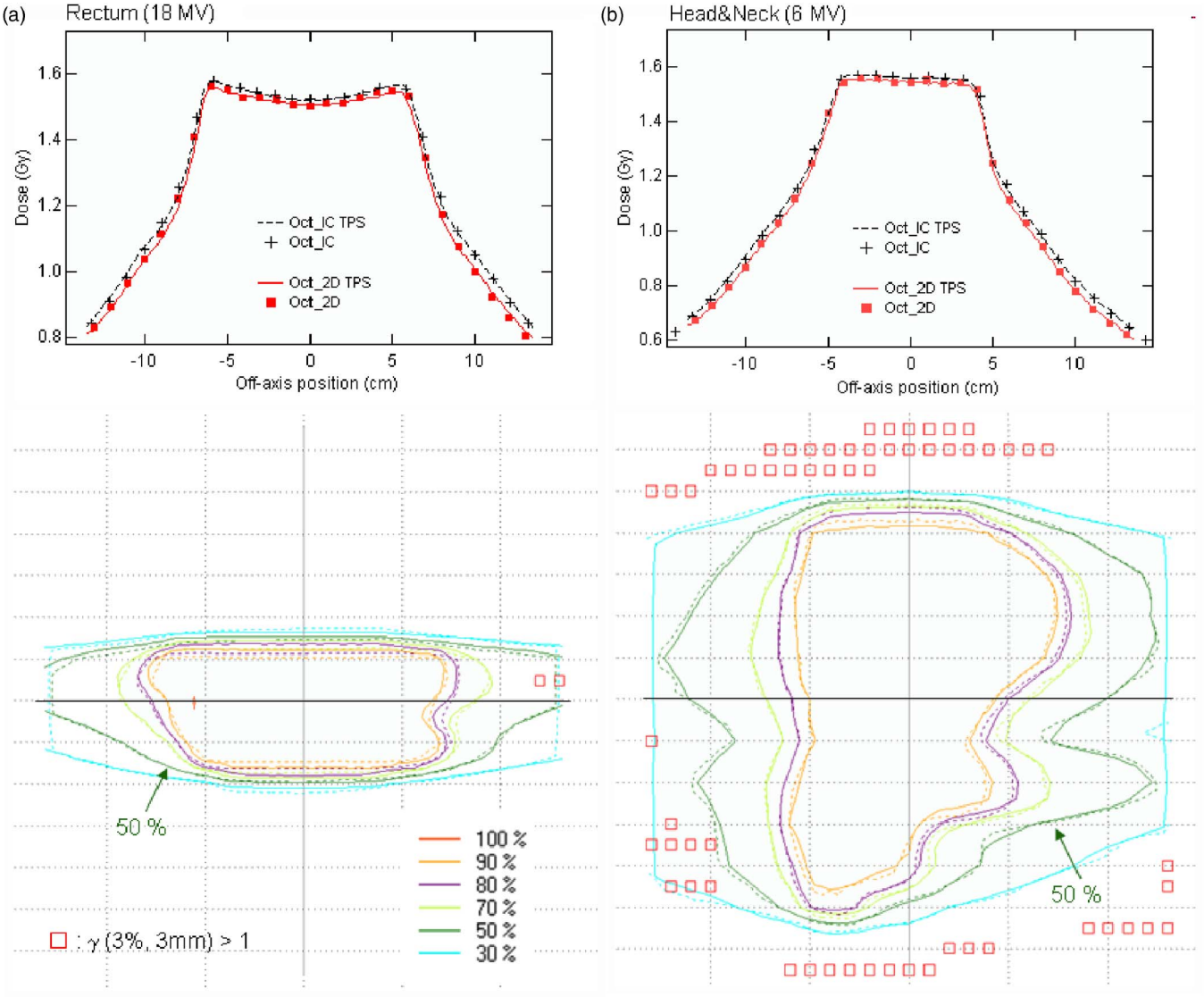

FIG. 8. Typical results obtained during patient plan [(a) rectum (18 MV), (b) head and neck (6 MV)] verification of dynamic MLC arc treatments. The upper part of the figure shows data obtained with the multiple ion chamber insert (Oct_IC) and data extracted from the 2D array data (Oct_2D). The lower part displays the result of the gamma evaluation, superposed on the isodose overlay. The red squares indicate the measurement points for which the gamma evaluation (3%, 3 mm) was out of tolerance. The arrow indicates the 50% isodose level. The solid line indicates the location of the displayed line profile.

entirely be canceled out. When measuring a 3D dose delivery, however, choosing the correct plane for the dose export becomes more critical than in the orthogonal geometry as high dose gradients may cause the dose in nearby planes to differ substantially. As the effective plane of measurement was found to lie in the central plane through the ion chambers (regardless of the beam incidence) instead of at the upper electrode, corrective action needed to be undertaken with respect to the absolute calibration factor. All further measurements took the energy dependent correction factors (0.981 for 6 MV, 0.985 for 18 MV) into account.

The 2D ion chamber array shows a relatively simple directional dependence. When irradiated from the rear, the collected charge is 4% (18 MV) and 8% (6 MV) lower than when irradiated from the front, for orthogonal as well as oblique beam incidences. Only a short transition period is observed for sidewise irradiation before these constant values are obtained. As an ion chamber measurement in solid water showed that the array structure has a mean density that is nearly water equivalent (within 1.5%), the reduced charge collection cannot be attributed to additional dose absorbed by the backside detector construction. This reasoning was further supported by the dose calculations (AAA as well as collapsed cone) that predicted no more than 1% dose difference due to the additional amount of PMMA at the backside of the array. The reduced collection efficiency is inherent in the ion chamber construction and is most likely due to the use of materials with different atomic number Z for the upper and lower electrodes. Furthermore, it is worthwhile to mention that a dose calculation algorithm of sufficient accuracy with respect to heterogeneity correction is required. The AAA and collapsed cone dose calculation algorithms proved adequate, whereas the single pencil beam algorithm (Eclipse,

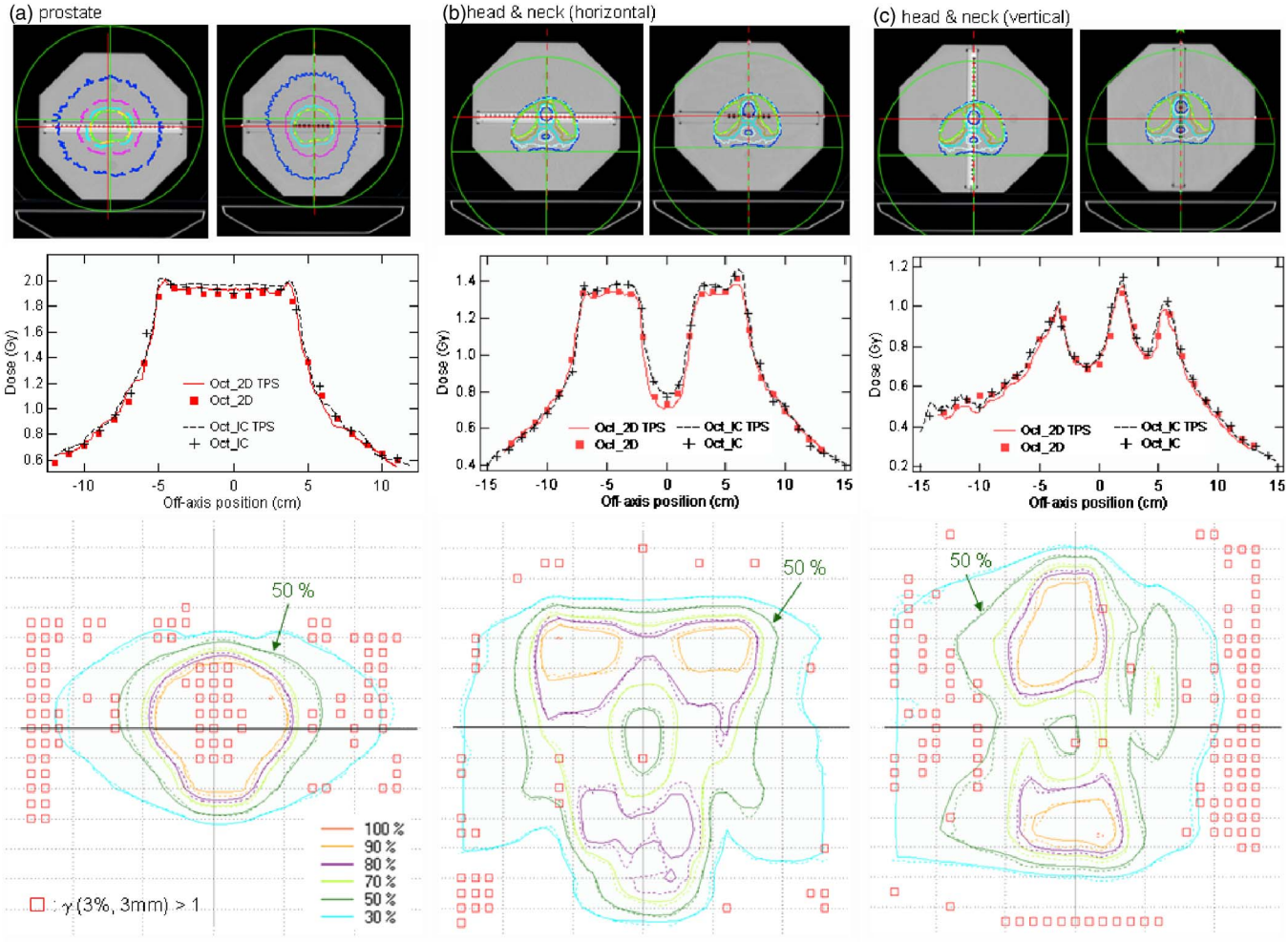

FIG. 9. Typical results obtained during patient plan verification on the TomoTherapy treatment unit. The upper part of the figure shows the phantom setups. The green lines indicate the center of the TomoTherapy unit. The red lines show the moveable lasers used for the phantom setup. The middle part of the figure shows data obtained with the multiple ion chamber insert (Oct_IC) and data extracted from the 2D array data (Oct_2D). The lower part displays the result of the gamma evaluation, superposed on the isodose overlay. The red squares indicate the measurement points for which the gamma evaluation (3%, 3 mm) is out of tolerance. The arrow indicates the 50% isodose level. The solid line indicates the location of the displayed line profile.

Varian Medical Systems) was unable to correctly predict the shoulders of the profiles in the longitudinal direction for oblique incidences (not shown).

IV.C. The Octavius^{729}/2D array QA tandem

The directional dependence of the collection efficiency of the array could adequately be accounted for by means of a compensation cavity as shown in Fig. 1(b). The reduced charge collection is balanced by the removal of the appropriate amount of phantom material. Although in theory, this compensation cavity should extend all the way up to the sides of the array, for practical reasons, it was solely manufactured below: Including a cavity in the phantom construction to the side of the array would have necessitated an increase in width of at least 6 cm, making the phantom too large and too bulky to handle. Deviations between calculation (AAA) and measurement therefore remain unaltered for sidewise beam incidence (~3% for 6 MV, ~2% for 18 MV). However, it should be mentioned that the dose calculation for these highly oblique sidewise beam angles requires extreme heterogeneity correction and should be regarded with a healthy amount of suspicion. (The same argument holds for the sidewise beam incidence of the multiple ion chamber insert.) When ignoring the uncertainties for these sidewise beam incidences, with Octavius$^{729}_{20}$ the anisotropic behavior is reduced to less than 1.5%. Important is the fact that calculations need to be performed on a CT scan of the Octavius$^{CT\text{-}IC}$ phantom without compensation cavity, while the Octavius$^{729}_{20}$ phantom is solely intended to be used during the actual measurement with the Seven29 2D ion chamber array. The agreement between dose calculation and measurements is within 2%, 3 mm for the multiple ion chamber and 2D array measurements of the simple half-arc open field deliveries on the Clinac.

Within the TomoTherapy solution, plans of equal simplicity could not be generated for both delivery and dose calculation but plan optimizations on geometrically simple target volumes were used as an alternative. The measurements on Octavius$^{729}_{20}$ with the 2D array and on Octavius$^{CT\text{-}IC}$ with the multiple ion chamber insert highlighted some areas of sub-

optimal agreement between calculation and delivery for the TomoTherapy solution. Measurements reveal a ~4% too low dose delivery in the center of the TomoTherapy treatment unit, gradually improving as the off-center distance increases. At 5 cm off-center distance, agreement is within 2%. The reason for these discrepancies is suspected to be suboptimal agreement between the preconfigured and actual beam profile of the treatment unit. As published by Langen *et al.*, the beam profile shape changes with the wear-out of the target: When normalizing beam profiles acquired over the course of seven weeks to their central value, they observed, e.g., a difference of ~5% at a 20 mm off-axis position. As the beam configuration in the Hi-Art TPS remains fixed, accurate agreement with the changing beam profile cannot be achieved during the whole lifetime of the target. However, even though changes in the shape and magnitude of the measured dose dip (Fig. 6) could indeed be observed over time, the discrepancy always remained visible, even immediately after a target change. We suspect that the preconfigured profile deviates from reality at any given moment in time. Therefore, the above described test plans clearly illustrate the need to not only verify the reproducibility of the beam profile, as is done during machine QA, but also to use simple verification plans that can be compared to the TPS dose calculation. Making dose calculation available for static gantry deliveries would provide a valuable asset for the physicist to verify the preconfigured beam data.

IV.D. Pre-treatment QA

When applying a correction factor for the daily machine output variation, excellent agreement (within 2%, 2 mm) between measurement (2D Array and multiple ion chambers) and calculation was obtained for dynamic MLC arc treatments within the Varian solution. The dynamic MLC movements used in this study were relatively simple, but the obtained results suggest that the Octavius^{729}/2D array tandem could also be an efficient QA tool for more highly (intensity) modulated arc therapy (IMAT) treatments (not yet available at our clinic). Although the measurement method would be identical, the obtained agreement may differ as complex MLC movements with small effective openings are not only more challenging to deliver, but the corresponding dose is also more difficult to calculate. Although the Octavius^{729}/2D array setup could also be used for the composite plan verification of a static gantry IMRT treatment, obtained results may be inferior to arc treatments when a substantial fraction of the dose is given through (nearly) lateral fields.

The use of the Octavius$^{729}_{20}$/2D array tandem on the TomoTherapy treatment unit, considerably facilitates pretreatment QA. Prior to every verification session, 5 to 10 min are required for the phantom setup, depending on whether or not an MV-CT is obtained for the phantom positioning. The time needed per 2D dose measurement is then simply the time required to deliver the treatment. Comparison with the calculated planar dose is performed on-line and takes less than 1 min. Unfortunately, for the planar dose export, a workaround needs to be used as the Hi-Art TPS was not designed to support 2D dose exports. Although this workaround is cumbersome, it does not increase the time for pretreatment QA by more than 1 min. For most patients acceptance criteria of 5%, 3 mm are met over the entire treatment field. Although 3%, 3 mm are more commonly used acceptance criteria for IMRT treatment verification, the decreased agreement between the 2D dose measurement and the 2D dose calculation export can have many causes. First, the suboptimal agreement seen in the cylindrical test plan in the center of the treatment beam is also expected to be present in the clinical treatment plans but less obvious to locate because of the high gradients and because of the fact that the center of the beam is not always in the center of the phantom during QA plan delivery. Second, as noticed during pretreatment daily machine QA, the absolute reproducibility of the TomoTherapy during the course of the measurements was of the order of 1%–2%, in agreement with the output stability of 1.75% reported by Chen *et al.*[38] Although the effect of output variations could be reduced in the displayed data by averaging over a number of data acquisitions, this is a highly time consuming procedure, not feasible in clinical routine. As a consequence, the machine output fluctuations are inherently present in pretreatment patient plan deliveries. Third, although one is evaluating a 3D dose delivery, the gamma evaluation is performed between two planar datasets. This is a sufficiently accurate procedure for field by field IMRT pretreatment QA, but when verifying a 3D dose delivery, small inaccuracies in either the selection of the export plane or in the measurement setup can deteriorate the gamma evaluation outcome. Ideally, a 3D dose export (not yet available) and 3D gamma calculation should therefore be used.

As already demonstrated during the daily QA session as part of the pretreatment patient QA, the Octavius^{729}/2D Array combination could potentially be used for the more elaborate TomoTherapy machine QA as well. A single phantom setup would speed up the QA procedure. The fact that all array measurements provide 2D absolute dose information increases their value and allows compacting of the QA procedures. Furthermore, the discrepancies observed in the center of the cylindrical dose delivery inspire caution when tuning the machine output to a single, central ion chamber measurement.

V. CONCLUSION

Although rotational radiotherapy treatments are increasingly used, the developed technology is still new and requires careful monitoring and verification. For the verification of these treatment methods, the Seven29 2D ion chamber array provides an overall accuracy comparable to that of single ion chamber measurements when it is used in combination with the Octavius$^{729}_{20}$ phantom. This phantom contains a compensation cavity to rectify the different collection efficiency when the array is irradiated from the rear. It should be used in combination with the Octavius$^{CT\text{-}IC}$ phantom for dose calculation. The latter is a multipurpose phantom that can also be used for multiple ion chamber measurements, heterogeneity correction verification, and CT cali-

bration. This QA method facilitates the pretreatment verification process by providing on-line absolute 2D dose information.

ACKNOWLEDGMENTS

The authors would like to thank PTW (Freiburg, Germany) for their support and for providing dosimetric equipment. Special thanks should be attributed to Dr. Bernd Allgaier and Dr. Edmund Schule for their enthusiasm and fruitful scientific contributions. A research grant from TomoTherapy, Inc. (Madison, WI) was given to Clinique Ste Elisabeth, Namur. 7Sigma has a research collaboration with Varian Medical Systems. The authors also wish to thank Nigel Wellock from Barts and London for providing them with the tissue equivalent heterogeneous inserts and Fabrice Feuillen for his assistance with the numerous CT scans.

[a]Author to whom correspondence should be addressed. Electronic mail: ann.vanesch@7sigma.be

[1]C. X. Yu, "Intensity-modulated arc therapy with dynamic multileaf collimation: An alternative to TomoTherapy," Phys. Med. Biol. **40**, 1435–1449 (1995).
[2]L. Ma, C. X. Yu, M. Earl, T. Holmes, M. Sarfaraz, X. A. Li, D. Shepard, P. Amin, S. DiBiase, M. Suntharalingam, and C. Mansfield, "Optimized intensity-modulated arc therapy for prostate cancer treatment," Int. J. Cancer **96**, 379–384 (2001).
[3]C. X. Yu, X. A. Li, L. Ma, D. Chen, S. Naqvi, D. Shepard, M. Sarfaraz, T. W. Holmes, M. Suntharalingam, and C. M. Mansfield, "Clinical implementation of intensity-modulated arc therapy," Int. J. Radiat. Oncol., Biol., Phys. **53**, 453–463 (2002).
[4]E. Wong, J. Z. Chen, and J. Greenland, "Intensity-modulated arc therapy simplified," Int. J. Radiat. Oncol., Biol., Phys. **53**, 222–235 (2002).
[5]M. A. Earl, D. M. Shepard, S. Naqvi, X. A. Li, and C. X. Yu, "Inverse planning for intensity-modulated arc therapy using direct aperture optimization," Phys. Med. Biol. **48**, 1075–1089 (2003).
[6]G. Bauman, E. Gete, J. Z. Chen, and E. Wong, "Simplified intensity-modulated arc therapy for dose escalated prostate cancer radiotherapy," Med. Dosim. **29**, 18–25 (2004).
[7]W. Duthoy, W. De Gersem, K. Vergote, T. Boterberg, C. Derie, P. Smeets, C. De Wagter, and W. De Neve, "Clinical implementation of intensity-modulated arc therapy (IMAT) for rectal cancer," Int. J. Radiat. Oncol., Biol., Phys. **60**, 794–806 (2004).
[8]D. M. Shepard, D. Cao, M. K. N. Afghan, and M. A. Earl, "An arc-sequencing algorithm for intensity modulated arc therapy," Med. Phys. **34**, 464–470 (2007).
[9]N. L. Childress, L. Dong, and I. I. Rosen, "Rapid radiographic film calibration for IMRT verification using automated MLC fields," Med. Phys. **29**, 2384–2390 (2002).
[10]M. Bucciolini, F. B. Buonamici, and M. Casati, "Verification of IMRT fields by film dosimetry," Med. Phys. **31**, 161–168 (2004).
[11]H. Mota, C. Sibata, S. Sasidharan, K. White, M. Wolfe, T. Jenkins, R. Patel, and R. Allison, "Improved calibration method of EDR films for IMRT-QA," Med. Phys. **32**, 1983 (2005).
[12]C. Fiandra, U. Ricardi, R. Ragona, S. Anglesio, F. R. Giglioli, E. Calamia, and F. Lucio, "Clinical use of EBT model GafchromicTM film in radiotherapy," Med. Phys. **33**, 4314–4319 (2006).
[13]L. Dong, J. Antolak, M. Salephour, K. Forster, L. O'Neill, R. Kendall, and I. Rosen, "Patient-specific point dose measurement for IMRT monitor unit verification," Int. J. Radiat. Oncol., Biol., Phys. **56**, 867–877 (2003).
[14]H. Gustavsson, A. Karlsson, S. A. Back, L. E. Olsson, P. Haraldsson, P. Engstrom, and H. Nystrom, "MAGIC-type polymer gel for three-dimensional dosimetry: Intensity-modulated radiation therapy verification," Med. Phys. **30**, 1264–1271 (2003).
[15]K. Vergote, Y. De Deene, W. Duthoy, W. De Gersem, W. DeNeve, E. Achten, and C. De Wagter, "Validation and application of polymer gel dosimetry for the dose verification of an intensity-modulated arc therapy (IMAT) treatment," Phys. Med. Biol. **49**, 287–305 (2004).
[16]T. R. Mackie, T. Holmes, S. Swerdloff, P. Reckwerdt, J. O. Deasy, J. Yang, B. Paliwal, and T. Kinsella, "TomoTherapy: A new concept for the delivery of dynamic conformal radiotherapy," Med. Phys. **20**, 1709–1719 (1993).
[17]T. R. Mackie, J. Balog, K. Ruchala, D. Shepard, S. Aldridge, E. Fitchard, P. Reckwerdt, G. Olivera, T. McNutt, and M. Mehta, "TomoTherapy," Semin. Radiat. Oncol. **9**, 108–117 (1999).
[18]M. Al-Ghazi, R. Kwon, J. Kuo, N. Ramsinghani, and R. Yakoob, "The University of California, Irvine experience with TomoTherapy using the Peacock system," Med. Dosim. **26**, 17–27 (2001).
[19]J. S. Welsh, R. R. Patel, M. A. Ritter, P. M. Harari, T. R. Mackie, and M. P. Mehta, "Helical TomoTherapy: An innovative technology and approach to radiation therapy," Technol. Cancer Res. Treat. **1**, 311–316 (2002).
[20]A. W. Beavis, "Is TomoTherapy the future of IMRT?" Br. J. Radiol. **77**, 285–295 (2004).
[21]D. A. Low, K. K. S. C. Chao, S. Mutic, R. L. Gerber, C. A. Perez, and J. A. Purdy, "Quality assurance of serial TomoTherapy for head and neck patient treatments," Int. J. Radiat. Oncol., Biol., Phys. **42**, 681–692 (1998).
[22]J. Balog, T. Holmes, and R. Vaden, "A helical TomoTherapy dynamic quality assurance," Med. Phys. **33**, 3939–3950 (2006).
[23]J. D. Fenwick, W. A. Tomé, H. A. Jaradat, S. K. Hui, J. A. James, J. P. Balog, C. N. DeSouza, D. B. Lucas, G. H. Olivera, T. R. Mackie, and B. R. Paliwal, "Quality assurance of a helical TomoTherapy machine," Phys. Med. Biol. **49**, 2933–2953 (2004).
[24]K. M. Langen, S. L. Meeks, D. O. Poole, T. H. Wagner, T. R. Willoughby, O. A. Zeidan, P. A. Kupelian, K. J. Ruchala, and G. H. Olivera, "Evaluation of a diode array for QA measurements on a helical TomoTherapy unit," Med. Phys. **32**, 3424–3430 (2005).
[25]P. B. Greer and C. C. Popescu, "Dosimetric properties of an amorphous silicon electronic portal imaging device for verification of dynamic intensity modulated radiation therapy," Med. Phys. **30**, 1618–1627 (2003).
[26]B. Warkentin, S. Steciw, S. Rathee, and B. G. Fallone, "Dosimetric IMRT verification with a flat-panel EPID," Med. Phys. **30**, 3143–3155 (2003).
[27]A. Van Esch, T. Depuydt, and D. P. Huyskens, "The use of an a Si-based EPID for routine absolute dosimetric pretreatment verification of dynamic IMRT fields," Radiother. Oncol. **71**, 223–234 (2004).
[28]E. Spezi, A. L. Angelini, F. Romani, and A. Ferri, "Characterization of a 2D ion chamber array for the verification of radiotherapy treatments," Phys. Med. Biol. **50**, 3361–3373 (2005).
[29]B. Poppe, A. Blechschmidt, A. Djouguela, R. Kollhoff, A. Rubach, K. C. Willborn, and D. Harder, "Two-dimensional ionization chamber arrays for IMRT plan verification," Med. Phys. **33**, 1005–1015 (2006).
[30]A. Van Esch, L. Tillikainen, J. Pyykkonen, M. Tenhunen, H. Helminen, S. Siljamäki, J. Alakuijala, M. Paiusco, M. Iori, and D. P. Huyskens, "Testing of the analytical anisotropic algorithm for photon dose calculation," Med. Phys. **33**, 4130–4147 (2006).
[31]J. M. Lydon, "Photon dose calculations in homogeneous media for a treatment planning system using a collapsed cone superposition convolution algorithm," Phys. Med. Biol. **43**, 1813–1822 (1998).
[32]M. R. Arnfield, C. H. Siantar, J. Siebers, P. Garmon, L. Cox, and R. Mohan, "The impact of electron transport on the accuracy of computed dose," Med. Phys. **27**, 1266–1274 (2000).
[33]M. Miften, M. Wiesmeyer, S. Monhofer, and K. Krippner, "Implementation of FFT convolution and multigrid superposition models in the FOCUS RTP system," Phys. Med. Biol. **45**, 817–833 (2000).
[34]M. M. Aspradakis, R. Morrison, N. Richmond, and A. Steele, "Experimental verification of convolution/superposition photon dose calculations for radiotherapy treatment planning," Phys. Med. Biol. **48**, 2873–2893 (2003).
[35]D. A. Low, W. B. Harms, M. Sasa, and J. A. Purdy, "A technique for the quantitative evaluation of dose distributions," Med. Phys. **25**, 656–661 (1998).
[36]T. Depuydt, A. Van Esch, and D. P. Huyskens, "A quantitative evaluation of IMRT distributions: Refinement and clinical assessment of the gamma evaluation," Radiother. Oncol. **62**, 309–319 (2002).
[37]W. Lu, G. H. Olivera, M. L. Chen, P. J. Reckwerdt, and T. R. Mackie, "Accurate convolution/superposition for multi-resolution dose calculation using cumulative tabulated kernels," Phys. Med. Biol. **50**, 655–680 (2005).
[38]C. Chen, J. Meadows, and T. Bichay, "TomoDose: A daily quality assurance device for helical TomoTherapy," Med. Phys. **33**, 2207 (2006).